



UNIVERSITÀ DI PARMA

ARCHIVIO DELLA RICERCA

University of Parma Research Repository

An in silico structural approach to characterize human and rainbow trout estrogenicity of mycotoxins: Proof of concept study using zearalenone and alternariol

This is the peer reviewed version of the following article:

Original

An in silico structural approach to characterize human and rainbow trout estrogenicity of mycotoxins: Proof of concept study using zearalenone and alternariol / Dellaflora, L.; Oswald, I. P.; Dorne, J. -L.; Galaverna, G.; Battilani, P.; Dall'Asta, C.. - In: FOOD CHEMISTRY. - ISSN 0308-8146. - 312:(2020), p. 126088. [10.1016/j.foodchem.2019.126088]

Availability:

This version is available at: 11381/2871226 since: 2022-01-18T22:56:12Z

Publisher:

Elsevier Ltd

Published

DOI:10.1016/j.foodchem.2019.126088

Terms of use:

Anyone can freely access the full text of works made available as "Open Access". Works made available

Publisher copyright

note finali coverpage

(Article begins on next page)

Manuscript Number: FOODCHEM-D-19-02555R1

Title: An in silico structural approach to characterize human and rainbow trout estrogenicity of mycotoxins: Proof of concept study using zearalenone and alternariol

Article Type: Research Article (max 7,500 words)

Keywords: mycotoxins, zearalenone, alternariol, estrogen receptors, in silico toxicology, toxicodynamic

Corresponding Author: Dr. Luca Dellafiora, Ph.D.

Corresponding Author's Institution: University of Parma

First Author: Luca Dellafiora, Ph.D.

Order of Authors: Luca Dellafiora, Ph.D.; Isabelle P Oswald; Jean-Lou Dorne; Gianni Galaverna; Paola Battilani; Chiara Dall'Asta

Abstract: The mycotoxins zearalenone and alternariol may contaminate food and feed raising toxicological concerns due to their estrogenicity. Inter-species differences in their toxicokinetics and toxicodynamics may occur depending on evolution of taxa-specific traits. As a proof of principle, this manuscript investigates the comparative toxicodynamics of zearalenone, its metabolites (alpha-zearalenol and beta-zearalenol), and alternariol with regards to estrogenicity in humans and rainbow trout. An in silico structural approach based on docking simulation, pharmacophore modeling and molecular dynamics was applied and computational results were analyzed in comparison with available experimental data. The differences of estrogenicity among species of zearalenone and its metabolites have been structurally explained. Also, the low estrogenicity of alternariol in trout has been characterized here for the first time. This approach can provide a powerful tool for the characterization of interspecies differences in mycotoxin toxicity for a range of protein targets and relevant compounds for the food-and feed-safety area.

1 **An *in silico* structural approach to characterize human and rainbow trout estrogenicity of**
2 **mycotoxins: Proof of concept study using zearalenone and alternariol**

3

4 Luca Dellafiora^{1*}, Isabelle P. Oswald², Jean-Lou Dorne³, Gianni Galaverna¹, Paola Battilani⁴,
5 Chiara Dall'Asta¹

6

7 ¹ Department of Food and Drug, University of Parma, Area Parco delle Scienze 27/A, 43124
8 Parma, Italy

9 ² Toxalim (Research Centre in Food Toxicology), Université de Toulouse, INRA, ENVT, INP-
10 Purpan, UPS, 31027 Toulouse, France

11 ³ European Food Safety Authority (EFSA),

12 ⁴ Department of sustainable crop production, Università Cattolica del Sacro Cuore, Via Emilia
13 Parmense 84, 29122 Piacenza, Italy

14

15

16

17 * Correspondence to:

18 Luca Dellafiora. Department of Food and Drug, University of Parma, Area Parco delle Scienze
19 27/A, 43124 Parma, Italy. Phone: +390521906196. Email: luca.dellafiora@unipr.it

20

21 Authors email: Luca Dellafiora, luca.dellafiora@unipr.it; Isabelle P. Oswald,
22 isabelle.oswald@inra.fr; Jean-Lou Dorne, Jean-Lou.DORNE@efsa.europa.eu; Gianni Galaverna,
23 gianni.galaverna@unipr.it; Paola Battilani, paola.battilani@unicatt.it; Chiara Dall'Asta,
24 chiara.dallasta@unipr.it

25 **Abstract**

26 The mycotoxins zearalenone and alternariol may contaminate food and feed raising toxicological
27 concerns due to their estrogenicity. Inter-species differences in their toxicokinetics and
28 toxicodynamics may occur depending on evolution of taxa-specific traits. As a proof of principle,
29 this manuscript investigates the comparative toxicodynamics of zearalenone, its metabolites
30 (alpha-zearalenol and beta-zearalenol), and alternariol with regards to estrogenicity in humans
31 and rainbow trout. An *in silico* structural approach based on docking simulation, pharmacophore
32 modeling and molecular dynamics was applied and computational results were analyzed in
33 comparison with available experimental data. The differences of estrogenicity among species of
34 zearalenone and its metabolites have been structurally explained. Also, the low estrogenicity of
35 alternariol in trout has been characterized here for the first time. This approach can provide a
36 powerful tool for the characterization of interspecies differences in mycotoxin toxicity for a
37 range of protein targets and relevant compounds for the food-and feed-safety area.

38

39

40 *Keywords:* mycotoxins, zearalenone, alternariol, estrogen receptors, in silico toxicology,
41 toxicodynamic

42 **1. Introduction**

43 Zearalenone (ZEN) belongs to a group of mycotoxins of public and animal health concern due to
44 its distribution worldwide, the frequencies and the levels of contamination in food and feed, and
45 the severity of adverse effects it may evoke in living organisms (Dong, Pan, Wang, Ahmed, Liu,
46 Peng, et al., 2018). From a chemical point of view, ZEN is a low-molecular weight secondary
47 metabolite produced by fungi belonging to *Fusarium spp.*, mainly *F. culmorum* and *F.*
48 *graminearum* (Marin, Ramos, Cano-Sancho, & Sanchis, 2013). It is chemically described as 6-
49 (10-hydroxy-6-oxo-trans-1-undecenyl)-beta-resorcylic acid lactone (Figure 1). ZEN, along with
50 a number of cognate metabolites, can be found as contaminant in small grains, maize and derived
51 products. The reduced metabolites α -zearalenol and β -zearalenol (α ZEL and β ZEL, respectively)
52 are among the most abundant forms co-occurring with ZEN (Gromadzka, Waskiewicz,
53 Chelkowski, & Golinski, 2008), though they may be produced significantly also by the phase I
54 metabolism of mammals (EFSA, 2011). Besides evidences pointing to cytotoxic and genotoxic
55 effects, ZEN and its metabolites pose a health risk for humans and animals mainly on account of
56 their xenoestrogenic activity (EFSA, 2011). The main molecular mechanism underlying
57 estrogenicity of ZEN and its metabolites requires the direct binding and activation of estrogen
58 receptors (ERs), which are ligand-induced intracellular transcriptional factors belonging to the
59 nuclear receptor superfamily (Brzozowski, Pike, Dauter, Hubbard, Bonn, Engström, et al., 1997;
60 Spyraakis & Cozzini, 2009).

61 Several research efforts have described marked interspecies differences in terms of susceptibility
62 to the stimulation by ZEN and its metabolites (EFSA, 2017). In this respect, pigs are amongst the
63 most sensitive species (Binder, Schwartz-Zimmermann, Varga, Bichl, Michlmayr, Adam, et al.,
64 2017), while chicken are more resistant (Pitt, 2013). Inter-species differences in the toxicokinetic

65 profiles of ZEN and its metabolites in animal species have been recognized as the rationale
66 behind species susceptibility and sensitivity (EFSA, 2017; Mally, Solfrizzo, & Degen, 2016;
67 Zinedine, Soriano, Moltó, & Mañes, 2007). Specifically, sensitive species primarily produce
68 metabolites with larger estrogenic potency compared with ZEN and this has been demonstrated
69 for the phase-I metabolite α ZEL (Binder, et al., 2017). Conversely, species that are more
70 resistant to the toxicity of ZEN tend to produce larger amount of metabolites with estrogenic
71 potency lower than that from ZEN such as the phase I metabolite β ZEL (Devreese, Antonissen,
72 Broekaert, De Baere, Vanhaecke, De Backer, et al., 2015). However, interspecies differences in
73 toxicokinetics (TK) may not fully account for species susceptibility and sensitivity to ZEN and
74 toxicodynamic (TD) differences may also play a role in sensitivity among species, though they
75 are not commonly considered. In this regard, inter-species differences in the primary sequences
76 of estrogen receptors (ERs) may impact binding of ZEN and its metabolites, with subsequent
77 consequences on ERs activation and estrogenic potency (Matthews, Celius, Halgren, &
78 Zacharewski, 2000). In the context of risk assessment, the molecular characterization of such TD
79 differences may provide precious information to better understand the species-specific
80 mechanisms of toxicity and to provide a more through explanation of inter-species differences.
81 This manuscript deals with the comparative modelling of the estrogenic activity of ZEN, α ZEL
82 and β ZEL in human and rainbow trout (*Oncorhynchus mykiss*) to investigate interspecies
83 differences as a proof of principle. To do so, a computational workflow based on molecular
84 modelling techniques has been used. Notably, computational methods provides valuable tools for
85 the characterization of biological and toxicological properties of a wide spectrum of molecules
86 (e.g. (Cheron, Casciuc, Golebiowski, Antonczak, & Fiorucci, 2017; L. Dellafiora, Dall'Asta,
87 Cruciani, Galaverna, & Cozzini, 2015; Ivanova, Karelson, & Dobchev, 2018; Lin, Zhang, Han,

88 Xin, Meng, Gong, et al., 2018)).

89 In addition, the estrogenic potential of alternariol (AOH), an emerging mycotoxin with
90 estrogenic properties produced by *Alternaria spp.* (L. Dellafiora, Warth, Schmidt, Del Favero,
91 Mikula, Fröhlich, et al., 2018), has also been assessed. Deepening the understanding of the
92 molecular aspects of ZEN and AOH estrogenicity in trout is also very relevant given the overall
93 paucity of data and the poor understanding of mycotoxins action in fish, even though a number
94 of mycotoxins, including ZEN and AOH, constitute emerging hazards to fish health in rivers and
95 modern aquaculture (Gonçalves, Schatzmayr, Albalat, & Mackenzie, 2018; Tolosa, Font, Manes,
96 & Ferrer, 2014).

97 In this context, the computational study presented here applies a workflow based on
98 pharmacophoric modelling, docking simulation and molecular dynamics, which has already
99 demonstrated to reliably model bioactivity and toxicity of low-molecular weight compounds (e.g.
100 ref. (L. Dellafiora, Dall'Asta, Cruciani, Galaverna, & Cozzini, 2015)). Specifically, this work
101 aims to: i) Model at the molecular level the diverse inter-species toxicodynamics of ZEN, α ZEL
102 and β ZEL with regards to their interaction with ERs using a structural approach. In this respect,
103 the computational modeling may be a rapid and cost-effective analytical method to valuably
104 integrate data from *in vitro* and *in vivo* trials in the risk assessment process (L. Dellafiora,
105 Dall'Asta, & Galaverna, 2018; Lewis, Kazantzis, Fishtik, & Wilcox, 2007). ii) Characterize inter-
106 species differences in ERs binding to provide a mechanistic understanding of ZEN-related
107 effects among species. iii) Extend knowledge of the interspecies differences in AOH toxicity,
108 which is considered among the emerging mycotoxins of most concern (Gruber-Dorninger,
109 Novak, Nagl, & Berthiller, 2017).

110

111 **2. Materials and methods**

112 **2.1. Design of the human and rainbow trout estrogen receptor models**

113 The model of the alpha isoform of human ER (hER α) ligand binding domain was designed from
114 the ZEN-bound crystallographic structure deposited in the RCSB PDB databank
115 (<http://www.rcsb.org>) with ID code 5KRC (chain A) (Nwachukwu, Srinivasan, Bruno, Nowak,
116 Wright, Minutolo, et al., 2017). The structure was processed using the Sybyl software, version
117 8.1 (www.certara.com) checking the consistency of atom and bond types assignment and
118 removing the co-crystallised ligand and waters, as previously reported (L. Dellafiora, Galaverna,
119 Dall'Asta, & Cozzini, 2015). The protein presented unresolved coordinates in the regions 332-
120 335 and 461-472. The sequence continuity in the region 461-472 was achieved using the “Align
121 Structure by Homology” tool of the Biopolymer module of Sybyl software, version 8.1
122 (www.certara.com) by superimposing the human ER α structure with PDB code 2YJA (Phillips,
123 Roberts, Schade, Bazin, Bent, Davies, et al., 2011) and linking to the model the corresponding
124 atomic coordinates of such region. Conversely, the continuity of the region 332-335 was
125 achieved using the Loop/Refine module of Modeler software (version 9.1) (Sali & Blundell,
126 1993) interfaced in the UCSF Chimera software (version 1.11) (Pettersen, Goddard, Huang,
127 Couch, Greenblatt, Meng, et al., 2004) limiting the structure refinements at the missing part only.
128 The number of models to generate was set at five and only the best scored model according to
129 GA341 and zDOPE scores was considered.

130 Since no rainbow trout ER (rtER) structures were available in the PDB databank
131 (<http://www.rcsb.org>) (last database access in January 17th, 2019), the 3D model of the rainbow
132 trout ER α ligand binding domain (NCBI Reference Sequence: NP_001117821.1; residues 323-
133 560) was achieved through homology modeling using the hER model as a template, as

134 previously reported (L. Dellafiora, Dall'Asta, & Cozzini, 2015) within the software Modeler
135 (version 9.1) (Sali & Blundell, 1993) interfaced in the UCSF Chimera software (version 1.11)
136 (Pettersen, et al., 2004) . The root-mean square deviation (RMSD) analysis of proteins backbone
137 between trout model and its human template was done using the “Compare Structures” tool of
138 the Biopolymer module of Sybyl software, version 8.1 (www.certara.com).
139 For sequence analysis, the global pairwise alignment of ER ligand binding domains primary
140 sequence was conducted using the on-line tool EMBOSS-Water Pairwise Sequence Alignment
141 (<http://www.ebi.ac.uk>) and the Needleman-Wunsch alignment algorithm.

142 **2.2 Pharmacophoric modelling**

143 The binding site of both hER α and rtER α models was defined using the Flapsite tool of the
144 FLAP software together with the GRID algorithm to investigate the corresponding
145 pharmacophoric space (Baroni, Cruciani, Sciabola, Perruccio, & Mason, 2007; Carosati,
146 Sciabola, & Cruciani, 2004). The DRY probe was applied to describe potential hydrophobic
147 interactions, while the sp² carbonyl oxygen (O) and the neutral flat amino (N1) probes were used
148 to describe the hydrogen bond acceptor and donor capacity of the target, respectively.

149 **2.3 Docking simulations**

150 GOLD (Genetic Optimization for Ligand Docking) software was chosen to perform docking
151 studies as the appropriate tool for computing protein-ligand interactions (e.g. (Maldonado-Rojas
152 & Olivero-Verbel, 2011; Rollinger, Schuster, Baier, Ellmerer, Langer, & Stuppner, 2006)). The
153 occupancy of the binding site was set within a sphere 10 Å around the centroid of the pocket.
154 Software setting and docking protocol previously reported were used (L. Dellafiora, Galaverna,
155 & Dall'Asta, 2017). As an exception, the use of external scoring functions was omitted as the
156 GOLD's internal scoring function GOLDScore succeeded in analyzing the reference set of

157 compounds (*vide infra*). Specifically, GOLDScore fitness considers the external (protein-ligand
158 complex) and internal (ligand only) van der Waals energy, protein-ligand hydrogen bond energy
159 and ligand torsional strain energy. In each docking study, the proteins were kept semi-flexible
160 and the polar hydrogen atoms were set free to rotate. The ligands were set fully flexible.
161 GOLD implements a genetic algorithm that may introduce variability in the results. Therefore,
162 testing of the models were performed in triplicates and results were expressed as mean \pm
163 standard deviation (SD) ratio to the reference compound E2 to ensure causative scores
164 assignments for ER binding. In addition, molecules showing multiple poses and/or low and
165 variable score (coefficient of variation > 10%) were considered a priori unable to favorably bind
166 the pocket being unable to find a stable binding pose and were not included in the statistical
167 analysis (L Dellafiora, Galaverna, Cruciani, Dall'Asta, & Bruni, 2018).

168 **2.4 Molecular dynamic**

169 Molecular dynamic (MD) simulations were performed to investigate the dynamic of ligands
170 interaction with the ligand binding site of both human and trout ER, in comparison to those of
171 the endogenous agonist E2. The best scored binding poses calculated by docking simulation were
172 used as input for MD. MD simulations were performed using GROMACS (version 5.1.4)
173 (Abraham, Murtola, Schulz, Páll, Smith, Hess, et al., 2015) with CHARMM27 all-atom force
174 field parameters support (Best, Zhu, Shim, Lopes, Mittal, Feig, et al., 2012). All the ligands have
175 been processed and parameterized with CHARMM27 all-atom force field using the SwissParam
176 tool (<http://www.swissparam.ch>). Crystallographic waters kept in the docking studies were
177 removed and protein-ligand complexes were solvated with SPCE waters in a cubic periodic
178 boundary condition, and counter ions (Na^+ and Cl^-) were added to neutralize the system. Prior to
179 MD simulation, the systems were energetically minimized to avoid steric clashes and to correct

180 improper geometries using the steepest descent algorithm with a maximum of 5,000 steps.
181 Afterwards, all the systems underwent isothermal (300 K, coupling time 2psec) and isobaric (1
182 bar, coupling time 2 psec) 100 psec simulations before running 50 nsec simulations (300 K with
183 a coupling time of 0.1 psec and 1 bar with a coupling time of 2.0 psec).

184 **2.5 Statistical analysis**

185 Statistical analysis of docking results was performed using IBM SPSS Statistics for Linux,
186 version 25 (IBM Corp., Armonk, NY). The data was analysed by one-way ANOVA ($\alpha = 0.05$),
187 followed by post hoc Fisher's LSD test ($\alpha = 0.05$), except for the paired ratio comparisons that
188 were analyzed using paired student's t test.

189

190 **3. Results and Discussion**

191 **3.1 Design of trout ER model**

192 There are no 3D structures of rainbow trout ER available in the PDB databank
193 (<http://www.rcsb.org>) (last database access in January 17th, 2019). Therefore, the rainbow trout
194 ER (rbER) model was designed using homology modelling, a technique which can provide
195 reliable 3D models of biological targets when the structure of homologous proteins are available
196 (Lohning, Levonis, Williams-Noonan, & Schweiker, 2017; Monzon, Zea, Marino-Buslje, &
197 Parisi, 2017). Notably, homology modelling may be particularly suitable to model the ligand
198 binding domain of ERs given the strong conservation of 3D structures along the evolutionary
199 path of nuclear receptors, and especially among the ER orthologous (Pike, Brzozowski, &
200 Hubbard, 2000).

201 The alpha isoform of hER (hERa) was used as a template to model the alpha 1 isoform of rbER.

202 The hERa and rtER orthologous addressed in this study (GenBank accession code AAD52984.1,
203 residues 310-547; and NCBI reference sequence NP_001117821.1, residues 323-560,
204 respectively) shared 64 % of sequence identity and 81 % of sequence similarity (according to
205 BLOSUM62 matrix) respectively. To note, sequences sharing an identity higher than 50% are
206 typically though to provide high-confidence models (Dalton & Jackson, 2007). In addition, the
207 root-mean squared deviation (RMSD) analysis of proteins backbone between the model and its
208 template was done to further check the model confidence. The very low value recorded (0.74 Å)
209 pointed to the high confidence of the model used, in agreement with previous studies (Nikolaev,
210 Shtyrov, Panov, Jamal, Chakchir, Kochemirovsky, et al., 2018). With regards to the ligand
211 binding pockets, the sequence appeared highly conserved with the exception of L349/362M and
212 M528/541I substitutions (according to human and fish numeration, respectively) (Figure 2). The
213 geometrical reliability of rbER was checked comparing the model with the crystallographic
214 structures of hER. As shown in Figure 2, the overall geometrical organization of rbER was
215 correctly predicted in terms of ternary structure and in terms of arrangement of pocket
216 architecture and spatial distribution of residues, thereby supporting its use as reliable model for
217 the following analysis.

218 **3.2 Pharmacophoric modeling**

219 The pharmacophoric fingerprint of the human and trout ERs ligand binding domain pocket has
220 been computed using the FLAP software (further details are reported in Section 2.2). The
221 fingerprints of the two ER orthologous in terms of distribution of hydrophobic and hydrophilic
222 space appeared mainly hydrophobic with two polar patches at the two pocket terminus formed by
223 Glu353/366, Arg394/407 and His524/537, as previously described (L. Dellafiora, Galaverna,
224 Dall'Asta, & Cozzini, 2015). Nevertheless, the M528/541I mutation was observed causing a

225 slight pocket reshape that resulted into an extension of the hydrophobic space in hER in
226 comparison to rbER (Figure 2).

227 **3.3 Docking simulations**

228 Docking simulations may reliably assess the bioactivity/toxicity of small molecules, as
229 demonstrated previously (Maldonado-Rojas & Olivero-Verbel, 2011; Rollinger, Schuster, Baier,
230 Ellmerer, Langer, & Stuppner, 2006). In particular, molecular modeling approaches able to
231 estimate the capability of ligands to dock the ligand pocket of the ERs agonist conformation may
232 succeed in assessing their (xeno)estrogenic activity (L. Dellaflora, Galaverna, Dall'Asta, &
233 Cozzini, 2015; Ehrlich, Dellaflora, Mollergues, Dall'Asta, Serrant, Marin-Kuan, et al., 2015).
234 However, a fit-for-purpose feasibility assessment of both models was performed comparing the
235 experimental data of ZEN, α ZEL and β ZEL estrogenicity with the scores respectively calculated.
236 The endogenous ligand E2 and the estrogenically inactive β -sitosterol were taken as positive and
237 negative controls, respectively. In addition, the calculated poses of E2, ZEN and α ZEL were
238 compared to the crystallographic architectures available so far to assess the geometrical
239 reliability of models.

240 As reported in Table 1, the docking procedure reliably categorized the set of compounds in both
241 models, reflecting the capability to properly compute the different capability of molecules to
242 comply with the physico-chemical properties of the two ER pockets. In particular, the
243 estrogenically inactive β -sitosterol recorded negative scores in both models pointing to its
244 unsuitability to satisfy the physico-chemical requirements of pockets. In addition, the high
245 variability of scores (coefficient of variations $\geq 15\%$) suggested its incapability to stably arrange
246 into the ligand pocket. On this basis, it was deemed unable to dock the pocket of the agonist
247 conformation of ER and it was computed unlikely to act as ER agonist, in agreement with

248 experimental data (Matthews, Celius, Halgren, & Zacharewski, 2000). Conversely, E2, α ZEL,
249 ZEN and β ZEL recorded in both models high and positive scores that were significantly different
250 from each other ($p < 0.001$ according to Fisher'LSD post hoc) and properly ranked according to
251 experimental data.

252 It is worth noticing that the mycotoxins under analysis had a diverse sensitivity in the two
253 species under analysis (Table 1): while α ZEL showed an estrogenic potency comparably higher
254 than ZEN in the two species (4-fold and 5-fold higher than ZEN in human and trout,
255 respectively), β ZEL appeared much less potent in trout than in human (about 800-fold and 2-fold
256 weaker than ZEN in trout and human, respectively). From a semi-quantitative point of view, the
257 computational analysis reliably computed such differences, being the computed ZEN/ β ZEL
258 scores ratio significantly higher in trout than in human (i.e. 1.84 ± 0.01 and 1.28 ± 0.02 ,
259 respectively; $p < 0.001$). Conversely, the computed ZEN/ α ZEL scores ratios were not
260 statistically different between the two species (i.e. 0.96 ± 0.01 and 0.97 ± 0.00 in human and
261 trout, respectively; $p = 0.37$), pointing to a comparable relative activity in both systems, in
262 agreement with data reported in the literature (Le Guevel & Pakdel, 2001). Therefore, the
263 relative potency of α ZEL and β ZEL to ZEN could be reliably estimated in both species on the
264 basis of the scores respectively computed. Conversely, the relative potencies of ZEN and α ZEL
265 to E2 couldn't be modeled quantitatively in neither of the two species, even though the overall
266 potency rank of compounds was correctly predicted in both models. Indeed, according to
267 experimental data, the relative potency of ZEN or α ZEL to E2 was found higher in trout than in
268 human (namely, the estrogenicity of ZEN and α ZEL in comparison to E2 was found higher in
269 trout than in human) (Table 1). Therefore, the computed scores ratios of ZEN and α ZEL to E2
270 were expected to be higher in trout than in human, but it was recorded the opposite. This

271 outcome pointed to the incapability of models presented to correctly predict the quantitative
272 relative potency among different classes of compounds. This finding was in agreement with
273 previous data highlighting that this kind of approaches can be used in quantitative way whether
274 compounds share a strong structural correlation (L. Dellafiora, Dall'Asta, & Cozzini, 2015;
275 Ehrlich, et al., 2015). Conversely, in the case of structurally unrelated compounds, such as ZEN
276 group members and E2, computational scoring can provide a sound rank of potency but are
277 likely to fail in providing (semi)quantitatively reliable relative potency factors. With regards to
278 geometric reliability, the computed poses of E2, ZEN and α ZEL were found in strong agreement
279 with the architectures of binding reported by crystallographic studies in terms of pocket
280 occupancy and ligand orientation. This finding finally pointed to the geometrical reliability of
281 both human and trout models (Figure 3). On the basis of these results, both models appeared
282 reliable in predicting the potency rank and the binding geometry of compounds under analysis,
283 even though the relative potency factors could be modeled only within ZEN group.

284 Then, the binding poses of ZEN, α ZEL and β ZEL in the two models were inspected to
285 investigate the mechanistic basis of their respective activity and, in particular, to explain the
286 differences in terms of susceptibility to β ZEL stimulation between the two species. From the
287 human ER model, differences between ZEN, α ZEL and β ZEL, which all involved the same
288 binding pose resembling E2 (Figure 3), could be explained in terms of pocket fitting as discussed
289 elsewhere by Ehrlich and co-workers (Ehrlich, et al., 2015). For α ZEL, the presence of one
290 hydroxyl group with α isomerism in correspondence to the His524, instead of a ketone as for
291 ZEN, demonstrated to be a preferable feature to stably interact with the pocket, as previously
292 observed for steroid ligands (Sonneveld, Riteco, Jansen, Pieterse, Brouwer, Schoonen, et al.,
293 2006). Structurally, this finding was rationalized through the comparison of the binding poses of

294 α ZEL and E2, wherein the α -hydroxyl group of α ZEL superimposed the 18- β hydroxyl group of
295 E2 (Figure 3D). Conversely, the hydroxyl group with β isomerism of β ZEL likely superimposes
296 the α -hydroxyl group of 17 α -estradiol, which is known to cause a reduction of pocket fitting as
297 testified by the lower estrogenicity of 17 α -estradiol in comparison to E2 (Sonneveld, et al., 2006).
298 From the trout ER model, ZEN and α ZEL showed the same binding pose recorded in the human
299 model, in spite of the presence of two mutations occurring at the binding site (L349/362M and
300 M528/541I according to human and fish numeration, respectively). A different orientation was
301 found for β ZEL instead, as shown in Figure 3E. The slight pocket reshaping due to L349/362M
302 and M528/541I mutations induced β ZEL to adopt a pose rotated about 180° onto the longitudinal
303 axis of pseudo-symmetry. In this atypical orientation, the aromatic ring of β ZEL was prevented
304 from superimposing the aromatic ring of ZEN, α ZEL and E2. Given the strict orientation the
305 aromatic rings must adopt into the pocket, as reported by the huge number of crystallographic
306 data available so far, such an uncommon arrangement did not point to a plausibly relevant
307 capability of β ZEL to interact with the pocket. On this basis, the atypical ligand arrangement and
308 uncommon pocket occupancy might explain at least in part the lower capability of β ZEL to
309 trigger estrogenic stimuli in trout ER in comparison to the human orthologous.

310 With regards to AOH, in the human ER model the procedure correctly predicted the potency
311 rank as AOH which was scored below ZEN, in agreement with the lower estrogenic activity
312 reported in literature (Lehmann, Wagner, & Metzler, 2006). This data further confirmed the
313 procedure reliability in estimating the potency rank of compounds. Notably, to the best of our
314 knowledge, no data were available for the estrogenicity of AOH in trout and, as shown in Table
315 1, AOH was expected to be qualitatively less potent than ZEN with a lower calculated score. In
316 addition, the comparison between the calculated poses of AOH within the human and trout ER

317 revealed differences in the pocket occupancy (Figure 3F). Indeed, AOH adopted, within the
318 human ER model, an orientation similar to those shown by E2, ZEN and α ZEL, which has been
319 largely described by crystallographic studies as the one properly fitting ER pocket. Conversely,
320 AOH within the trout ER model showed an uncommon and distorted orientation that might
321 suggest its unsuitability to properly fit the ER pocket. On this basis, the interaction with the trout
322 ER model can be concluded less likely with a potentially low capability for estrogenic activities
323 in comparison to the interaction with the human ER.

324

325 **3.4 Molecular dynamics**

326 MD studies were performed to integrate the results of docking simulation with the analysis of
327 molecular movements of ERs upon ligands binding. MDs were performed for ER of both species
328 in complex with E2, taken as positive control, and ZEN and β ZEL in the attempt to understand
329 the molecular basis of inter-species differences to β ZEL stimulation. It was calculated also the
330 ER-AOH complex to gain structural insights on the mechanisms underlying the estrogenicity of
331 AOH in hER and to predict its potential effects on rbER (to the best of our knowledge no data
332 are available so far with regards to the estrogenic activity of AOH in trout). The trajectory of
333 | ligands and the ~~root-mean-square-analysis~~ (RMSD) of protein C-alpha and ligands' atomic
334 | coordinates were analyzed to measure the overall structural stability of complexes, which is
335 | crucial for determining the estrogenic activity of ligands (*vide infra*).

336 With regards to hER, as shown in Figure 4A, the complex with E2 was found the more stable
337 with fluctuations of slight intensity that pointed to the overall stability of hER-E2 complex.
338 Conversely, the complex with ZEN showed stable fluctuations resembling the ones of hER-E2
339 complex up to about 40 nsec of simulation while increasing the geometrical instability hereafter.

340 The RMSD of hER in complex with AOH or β ZEL started increasing much earlier than hER in
341 complex with ZEN. This finding might suggest that AOH and β ZEL are less suitable than ZEN
342 to stabilize the agonistic conformation of hER, providing a mechanistic explanation to the lower
343 estrogenic potency found experimentally (Le Guevel & Pakdel, 2001; Lehmann, Wagner, &
344 Metzler, 2006). With regards to ligands within hER complexes, the RMSD fluctuations were
345 found stable and almost comparable to each other (Figure 4B). In addition, the number of
346 hydrogen bonds seemed not relevant to discriminate the potency of ligands, though E2 showed
347 the highest number of long-lasting number of hydrogen bonds along the timeframe considered
348 (Figure 4C). On this basis, the overall stability of hER complex could be considered an important
349 parameter to explain the diverse estrogenicity of ligands under investigation being found related
350 to their potency: the more lasting the overall geometrical stability of hER, the more higher the
351 estrogenic potency of ligands. Keeping in mind that the model was derived from the
352 crystallographic structure of hER in the agonist conformation, this finding is in agreement with
353 the current understanding of hER biochemistry which describes the need to keep stable the
354 agonist conformation of ER to elicit ligand-dependent estrogenic stimuli (Ehrlich, et al., 2015;
355 Spyrakis & Cozzini, 2009).

356 With regards to the rbER, as shown in Figure 5, rbER in complex with E2, ZEN or β ZEL was
357 found overall stable and with comparable RMSD fluctuations. Conversely, the complex with
358 AOH was found more unstable showing an early (from 10 nsec) and marked RMSD increase. As
359 shown for hER, also in the case of rbER the number and lasting of hydrogen bonds was found
360 not directly correlated to the potency of ligands (Figure 5C). For the geometrical stability of
361 ligands, the RMSD fluctuations of ZEN, β ZEL and AOH were found more pronounced than the
362 ones of E2. In particular, β ZEL showed a drastic and discrete increase of RMSD in the second

363 part of the simulation. The close inspection of the binding poses revealed that such discrete
364 increase was due to a change in ligand orientation, as shown in Figure 5D. Notably, the
365 alternative conformation of β ZEL was supposed not complying with the structural requirements
366 of being a good ER ligand mainly due to the improper orientation of the aromatic ring that did
367 not retrace the common arrangement shown by crystallographic studies (Figure 5D). This
368 uncommon pocket occupancy might explain, at least in part, the lower activity of β ZEL in rbER
369 in comparison to its activity reported in hER (Le Guevel & Pakdel, 2001). Given the comparable
370 trend of RMSD fluctuations of rbER in complex with the various ligands, the C-alpha root-
371 mean-square fluctuation (RMSF) analysis was performed to check possible local differences in
372 the protein flexibility among the different rbER complexes studied. For the rbER- β ZEL complex
373 and using E2 as a reference, an increased local mobility of two key regions related to ER
374 activation was found among the regions showing differential mobility (Figure 5A). In particular,
375 one region included the residues 425-430, which belong to the so defined H8. That region is
376 proximal to the binding pocket and it was found previously related to the dissociation pathway of
377 ER ligands due to an enhanced local disordering (Sonoda, Martinez, Webb, Skaf, & Polikarpov,
378 2008). Therefore, the results collected in this work pointed to the weakness of β ZEL
379 estrogenicity with regards to its incapability to stabilize a long-lasting agonist-like organization
380 ER receptor and a dissociation pathway taking advantage of the increased disorder of H8 can be
381 hypothesized. The second region included the residues 549-557, which forms the so defined H12.
382 Notably, the proper ligand-dependent stabilization of H12 in the agonist conformation is crucial
383 for eliciting estrogenic activity (Brzozowski, et al., 1997; Spyrakis & Cozzini, 2009). Therefore,
384 a ligand-dependent disrupting action on the agonist-like stabilization of H12 likely relates with
385 non-agonistic activity, as shown for ER (partial) antagonists (Brzozowski, et al., 1997; Spyrakis

386 & Cozzini, 2009). On the basis of the results presented above, the markedly low activity of β ZEL
387 in rbER could be explained by multiple concerted molecular events. Among them, it could be
388 identified the improper pocket occupancy and the ligand-dependent enhancement of local protein
389 mobility that may facilitate β ZEL dissociation and/or impair the proper agonist conformation of
390 ER.

391 With regards to the ZEN-rbER complex, an increased disorder in comparison to E2 was
392 observed in the region 425-430, similarly to β ZEL. Also in this case, the dissociation pathway of
393 ZEN might take advantage of the increased mobility of such region. On the one hand, this
394 finding plausibly explained the lower activity of ZEN in comparison to E2 pointing to a less
395 lasting and more unstable interaction of ZEN with the pocket in comparison to the endogenous
396 ligand E2. On the other hand, the increased mobility of such region, but not in the region of H12,
397 as observed for β ZEL, provided a likely explanation to the different estrogenic activity the two
398 mycotoxins showed in rbER.

399 As a general remark, it is worth noticing the diverse effects that the set of ligands under analysis
400 exerted on the geometrical stability of ER orthologous. In the case of hER, ligands with different
401 potency exerted a clear and graded effect in the overall protein organization, providing a likely
402 rationale to understand mechanistically the diverse action they may have: the more they perturb
403 the stabilization of agonist conformation, the weaker their estrogenic potency is, in agreement
404 with the current understanding of ERs biochemistry (*vide infra*). Conversely, the overall
405 structure of the trout ER protein was found geometrically less affected by ligands than the human
406 orthologous (with the exception of AOH, which caused early disrupting effects on the overall
407 rbER structure; Figure 5). Indeed, in the case of rbER, ligands were found exerting subtle
408 conformational changes at a local level in key regions involved in protein activity rather than

409 disrupting the overall protein organization as observed for hER. This finding is in agreement
410 with the evolutionary biology of ER family and, more in general, with the nuclear receptor
411 super-family. Evolution has pushed nuclear receptors in the direction of being more ligand-
412 specific and more susceptible to ligand modulation (Bridgham, Eick, Larroux, Deshpande,
413 Harms, Gauthier, et al., 2010; Escriva, Delaunay, & Laudet, 2000). Keeping in mind that ERs
414 need to keep stable the agonist conformation to elicit estrogenic response (see above), the fine
415 ligand-dependent tuning inherently depends on the overall plasticity of receptors. Therefore,
416 proteins prone to relevant ligand-induced disorders as the consequence of slight changes on
417 ligands structure (as in the case of ZEN and its metabolites) are reasonably more selective than
418 those with an inherently more stable conformation. On the basis of the few data available so far,
419 rbER and hER, which underwent different evolutionary processes, showed an apparently
420 different ligand selectivity, with rbER showing a lower selectivity being able to bind ligands
421 encompassing a broader chemical space than hER (Matthews, Celius, Halgren, & Zacharewski,
422 2000). Therefore, the lower dependence of rbER from ligands in terms of overall geometrical
423 stability found in this study provided a reasonable explanation to the apparent diverse ligands
424 selectivity showed by the two ER orthologous in the few experimental trials available so far.

425 With regards to AOH, the rtER-AOH complex showed an early increase in RMSD values
426 pointing to the overall geometrical instability of the complex. In addition, the RMSF analysis
427 highlighted an increased mobility of the regions forming H8 and H12, as shown for β ZEL, and
428 an additional increased mobility in the region 385-397, which is part of the so defined H5. This
429 region surrounds the H12 and concurs, along with H12, to form the so defined AF2 surface
430 groove that mediate the recruitment of co-regulators protein underlying the full activation of ER
431 (Brzozowski, et al., 1997; Phillips, et al., 2011). Disorders in such regions relate to non-agonist

432 folding of ER (Spyrakis and Cozzini, 2009). Therefore, the concerted increases of structural
433 disorder in those regions led to hypothesize the strong agonistic behavior of AOH not likely. On
434 the basis of these results, a weak activity on the rbER accounted in this study could be
435 hypothesized for AOH. Nevertheless, further data need to be collected in the future on the
436 possible effects mediated by the other ER isoforms in order to precisely characterize the
437 estrogenic potency of AOH in trout.

438

439 4. Conclusion

440 ~~Interspecies differences in the TD of mycotoxins have been reported and can constitute a~~
441 ~~criterion for the categorization of living organisms into potentially susceptible or resistant~~
442 ~~species. The diverse health outcomes resulting from mycotoxin exposure among species~~
443 ~~inherently depend on the concerted variability in toxicokinetic and toxicodynamic processes~~
444 ~~amongst organisms as an intrinsic consequence of the specie's evolution. However, interspecies~~
445 ~~differences in TD are not always taken into account to explain the diversification of responses~~
446 ~~among different species, particularly for mycotoxins because comparative assessments have not~~
447 ~~been performed. Also, the molecular basis of the observed differences often remains unknown or~~
448 ~~only partially identified let alone characterized. In this context, integrating such toxicokinetic and~~
449 ~~toxicodynamic differences might lead to a better interpretation of toxicity data to move towards a~~
450 ~~more informed analysis and/or extrapolation of data between species. Hence, t~~The study
451 presented here addressed ~~the an inter-species~~ comparative analysis of toxicodynamic aspects of
452 mycotoxins, taking the estrogenicity of ZEN, α ZEL, β ZEL and AOH in human and trout as a
453 proof of principle. The study illustrated the reliability of using *in silico* structural approaches to

454 assess and understand the inter-species differences of mycotoxins toxicity from a toxicodynamic
455 perspective. Contextually, the study described the structural rationale behind the mechanisms of
456 action underlying the estrogenic activity of ZEN, α ZEL, β ZEL and AOH in human and trout.
457 Aside the different capability of these mycotoxins to bind and fit the two ER pockets, the
458 possible existence of species-specific structural changes of ER after mycotoxins binding has
459 been investigated. In particular, hER and rtER were found mainly affected by ligand-dependent
460 changes at a global and local level, respectively. With regards to β ZEL, a marked difference in
461 its docking capacity has been shown for the two ER orthologous. Specifically, the architecture of
462 binding calculated in the rtER did not match with the known binding mode characterized in
463 crystallographic studies. Therefore, the diverse capability to fit the ER pocket, along with the
464 differential disrupting effects on the agonist conformation of ER, provided a structural
465 explanation to the diverse potencies β ZEL may have on human and trout ER.
466 On the other hand, AOH, on the basis of all data collected, was considered unable to exert a
467 significant activity on the trout ER. Nevertheless, the thorough evaluation of possible activity on
468 the other ER isoforms, along with the assessment of any relevant AOH metabolite(s), should be
469 assessed critically in the future to provide a thorough molecular characterization of AOH action
470 on trout ER.

471 ~~In conclusion, structure-based molecular modeling approaches might provide a reliable, rapid~~
472 ~~and cost-effective early-warning system analysis to mechanistically study interspecies~~
473 ~~differences in TD of mycotoxins and other compounds. Such approaches will provide a useful~~
474 ~~analysis to complement the characterization of inter-species mycotoxins toxicity by: i)~~
475 ~~understanding the structural basis of mycotoxins toxicity; ii) predicting the capacity to~~
476 ~~differentially trigger biological and toxicological stimuli; iii) driving future analysis through the~~

477 ~~evidence-based prioritization of compounds, endpoints and species of interest to risk assessment;~~
478 ~~iv) integrating toxicokinetic data for a more comprehensive understanding of mycotoxins~~
479 ~~toxicity; v) supporting biologically based interpretation of toxicological data to improve~~
480 ~~extrapolation between species and the assessment of human relevance. In this light, studies~~
481 ~~investigating other classes of contaminants with known protein targets should be performed to~~
482 ~~calibrate tools and integrate them in a scientific workflow. This will allow the assessment of a~~
483 ~~broader diversity of biological and toxicological endpoints to assess the effective translation of~~
484 ~~this procedure in hazard and risk assessment of food and feed relevant chemicals.~~

485

486 **Acknowledgments**

487 The work was carried out as part of the MYCHIF EFSA project (GP/EFSA/AFSCO/2016/01).
488 The view expressed in this article are the authors only and do not necessarily represent the views
489 of the European Food Safety Authority. The authors acknowledge the CINECA award under the
490 ISCRA initiative, for the availability of high performance computing resources and support, and
491 Prof. Gabriele Cruciani for the courtesy of FLAP Software (www.moldiscovery.com).

492

493 **Conflict of interest**

494 The authors declare no conflict of interest.

495

496 **Reference**

- 497 Abraham, M. J., Murtola, T., Schulz, R., Páll, S., Smith, J. C., Hess, B., & Lindahl, E. (2015).
498 GROMACS: High performance molecular simulations through multi-level parallelism
499 from laptops to supercomputers *SoftwareX*, 1-2, 19-25.
- 500 Baroni, M., Cruciani, G., Sciabola, S., Perruccio, F., & Mason, J. S. (2007). A common reference
501 framework for analyzing/comparing proteins and ligands. Fingerprints for Ligands and
502 Proteins (FLAP): theory and application. *Journal of Chemical Information and Modeling*,
503 47(2), 279-294.
- 504 Best, R. B., Zhu, X., Shim, J., Lopes, P. E., Mittal, J., Feig, M., & Mackerell, A. D. J. (2012).
505 Optimization of the additive CHARMM all-atom protein force field targeting improved
506 sampling of the backbone ϕ , ψ and side-chain $\chi(1)$ and $\chi(2)$ dihedral angles. *Journal of*
507 *Chemical Theory and Computation*, 8(9), 3257-3273.
- 508 Binder, S. B., Schwartz-Zimmermann, H. E., Varga, E., Bichl, G., Michlmayr, H., Adam, G., &
509 Berthiller, F. (2017). Metabolism of Zearalenone and Its Major Modified Forms in Pigs.
510 *Toxins (Basel)*, 9(2), pii: E56.
- 511 Bridgman, J. T., Eick, G. N., Larroux, C., Deshpande, K., Harms, M. J., Gauthier, M. E. A.,
512 Ortlund, E. A., Degnan, B. M., & Thornton, J. W. (2010). Protein Evolution by
513 Molecular Tinkering: Diversification of the Nuclear Receptor Superfamily from a
514 Ligand-Dependent Ancestor. *Plos Biology*, 8(10).
- 515 Brzozowski, A. M., Pike, A. C., Dauter, Z., Hubbard, R. E., Bonn, T., Engström, O., Ohman, L.,
516 Greene, G. L., Gustafsson, J. A., & Carlquist, M. (1997). Molecular basis of agonism and
517 antagonism in the oestrogen receptor. *Nature*, 389(6652), 753-758.
- 518 Carosati, E., Sciabola, S., & Cruciani, G. (2004). Hydrogen bonding interactions of covalently

519 bonded fluorine atoms: from crystallographic data to a new angular function in the GRID
520 force field. *Journal of Medicinal Chemistry*, 47(21), 5114-5125.

521 Cheron, J. B., Casciuc, I., Golebiowski, J., Antonczak, S., & Fiorucci, S. (2017). Sweetness
522 prediction of natural compounds. *Food Chemistry*, 221, 1421-1425.

523 Dalton, J. A. R., & Jackson, R. M. (2007). An evaluation of automated homology modelling
524 methods at low target-template sequence similarity. *Bioinformatics*, 23(15), 1901-1908.

525 Dellafiora, L., Dall'Asta, C., & Cozzini, P. (2015). Ergot alkaloids: From witchcraft till in silico
526 analysis. Multi-receptor analysis of ergotamine metabolites. *Toxicology Reports*, 2, 535-
527 545.

528 Dellafiora, L., Dall'Asta, C., & Galaverna, G. (2018). Toxicodynamics of Mycotoxins in the
529 Framework of Food Risk Assessment-An In Silico Perspective. *Toxins*, 10(2), E52.

530 Dellafiora, L., Dall'Asta, C., Cruciani, G., Galaverna, G., & Cozzini, P. (2015). Molecular
531 Modelling approach to evaluate poisoning of topoisomerase I by alternariol derivatives.
532 *Food Chemistry*, 189, 93-101.

533 Dellafiora, L., Galaverna, G., Cruciani, G., Dall'Asta, C., & Bruni, R. (2018). On the Mechanism
534 of Action of Anti-Inflammatory Activity of Hypericin: An In Silico Study Pointing to the
535 Relevance of Janus Kinases Inhibition. *Molecules*, 23(12), piiE3058.

536 Dellafiora, L., Galaverna, G., & Dall'Asta, C. (2017). In silico analysis sheds light on the
537 structural basis underlying the ribotoxicity of trichothecenes - A tool for supporting the
538 hazard identification process. *Toxicology Letters*, 270, 80-87.

539 Dellafiora, L., Galaverna, G., Dall'Asta, C., & Cozzini, P. (2015). Hazard identification of
540 cis/trans-zearalenone through the looking-glass. *Food and Chemical Toxicology*, 86, 65-
541 71.

542 Dellafiora, L., Warth, B., Schmidt, V., Del Favero, G., Mikula, H., Fröhlich, J., & Marko, D.
543 (2018). An integrated in silico/in vitro approach to assess the xenoestrogenic potential of
544 *Alternaria* mycotoxins and metabolites. *Food Chemistry*, 248, 253-261.

545 Devreese, M., Antonissen, G., Broekaert, N., De Baere, S., Vanhaecke, L., De Backer, P., &
546 Croubels, S. (2015). Comparative Toxicokinetics, Absolute Oral Bioavailability, and
547 Biotransformation of Zearalenone in Different Poultry Species. *Journal of Agricultural*
548 *and Food Chemistry*, 63(20), 5092-5098.

549 Dong, G. L., Pan, Y. H., Wang, Y. L., Ahmed, S., Liu, Z. L., Peng, D. P., & Yuan, Z. H. (2018).
550 Preparation of a broad-spectrum anti-zearalenone and its primary analogues antibody and
551 its application in an indirect competitive enzyme-linked immunosorbent assay. *Food*
552 *Chemistry*, 247, 8-15.

553 EFSA. (2011). Scientific Opinion on the risks for public health related to the presence of
554 zearalenone in food. *EFSA J.*, 9, 2197.

555 EFSA. (2017). Risks for animal health related to the presence of zearalenone and its modified
556 forms in feed. *EFSA J.*, 15(7), 4851.

557 Ehrlich, V. A., Dellafiora, L., Mollergues, J., Dall'Asta, C., Serrant, P., Marin-Kuan, M., Lo
558 Piparo, E., Schilter, B., & Cozzini, P. (2015). Hazard assessment through hybrid in
559 vitro/in silico approach: The case of zearalenone. *ALTEX*, 32(4), 275-286.

560 Escriva, H., Delaunay, F., & Laudet, V. (2000). Ligand binding and nuclear receptor evolution.
561 *Bioessays*, 22(8), 717-727.

562 Gonçalves, R., Schatzmayr, D., Albalat, A., & Mackenzie, S. (2018). Mycotoxins in aquaculture:
563 feed and food. *Reviews in Aquaculture*, 0(0), 1-31.

564 Gromadzka, K., Waskiewicz, A., Chelkowski, J., & Golinski, P. (2008). Zearalenone and its

565 metabolites: occurrence, detection, toxicity and guidelines. *World Mycotoxins Journal*,
566 *1*(2), 209-220.

567 Gruber-Dorninger, C., Novak, B., Nagl, V., & Berthiller, F. (2017). Emerging Mycotoxins:
568 Beyond Traditionally Determined Food Contaminants. *Journal of Agricultural and Food*
569 *Chemistry*, *65*(33), 7052-7070.

570 Ivanova, L., Karelson, M., & Dobchev, D. A. (2018). Identification of Natural Compounds
571 against Neurodegenerative Diseases Using In Silico Techniques. *Molecules*, *25*(8), E1847.

572 Le Guevel, R., & Pakdel, F. (2001). Assessment of oestrogenic potency of chemicals used as
573 growth promoter by in-vitro methods. *Human Reproduction*, *16*(5), 1030-1036.

574 Lehmann, L., Wagner, J., & Metzler, M. (2006). Estrogenic and clastogenic potential of the
575 mycotoxin alternariol in cultured mammalian cells. *Food and Chemical Toxicology*,
576 *44*(3), 398-408.

577 Lewis, A., Kazantzis, N., Fishtik, I., & Wilcox, J. (2007). Integrating process safety with
578 molecular modeling-based risk assessment of chemicals within the REACH regulatory
579 framework: Benefits and future challenges. *Journal of Hazardous Materials*, *142*(3), 592-
580 602.

581 Lin, K., Zhang, L. W., Han, X., Xin, L., Meng, Z. X., Gong, P. M., & Cheng, D. Y. (2018). Yak
582 milk casein as potential precursor of angiotensin I-converting enzyme inhibitory peptides
583 based on in silico proteolysis. *Food Chemistry*, *254*, 340-347.

584 Lohning, A. E., Levonis, S. M., Williams-Noonan, B., & Schweiker, S. S. (2017). A Practical
585 Guide to Molecular Docking and Homology Modelling for Medicinal Chemists. *Current*
586 *Topics in Medicinal Chemistry*, *17*(18), 2023-2040.

587 Maldonado-Rojas, W., & Olivero-Verbel, J. (2011). Potential interaction of natural dietary

588 bioactive compounds with COX-2. *Journal of Molecular Graphics & Modelling*, 30, 157-
589 166.

590 Mally, A., Solfrizzo, M., & Degen, G. H. (2016). Biomonitoring of the mycotoxin Zearalenone:
591 current state-of-the art and application to human exposure assessment. *Archives of*
592 *Toxicology*, 90(6), 1281-1292.

593 Marin, S., Ramos, A. J., Cano-Sancho, G., & Sanchis, V. (2013). Mycotoxins: Occurrence,
594 toxicology, and exposure assessment. *Food and Chemical Toxicology*, 60, 218-237.

595 Matthews, J., Celius, T., Halgren, R., & Zacharewski, T. (2000). Differential estrogen receptor
596 binding of estrogenic substances: a species comparison. *The Journal of Steroid*
597 *Biochemistry and Molecular Biology*, 74(4), 223-234.

598 Monzon, A. M., Zea, D. J., Marino-Buslje, C., & Parisi, G. (2017). Homology modeling in a
599 dynamical world. *Protein Science*, 26(11), 2195-2206.

600 Nikolaev, D. M., Shtyrov, A. A., Panov, M. S., Jamal, A., Chakchir, O. B., Kochemirovsky, V.
601 A., Olivucci, M., & Ryazantsev, M. N. (2018). A Comparative Study of Modern
602 Homology Modeling Algorithms for Rhodopsin Structure Prediction. *Acs Omega*, 3(7),
603 7555-7566.

604 Nwachukwu, J. C., Srinivasan, S., Bruno, N. E., Nowak, J., Wright, N. J., Minutolo, F.,
605 Rangarajan, E. S., Izard, T., Yao, X. Q., Grant, B. J., Kojetin, D. J., Elemento, O.,
606 Katzenellenbogen, J. A., & Nettles, K. W. (2017). Systems Structural Biology Analysis
607 of Ligand Effects on ER alpha Predicts Cellular Response to Environmental Estrogens
608 and Anti-hormone Therapies. *Cell Chemical Biology*, 24(1), 35-45.

609 Pettersen, E. F., Goddard, T. D., Huang, C. C., Couch, G. S., Greenblatt, D. M., Meng, E. C., &
610 Ferrin, T. E. (2004). UCSF Chimera--a visualization system for exploratory research and

611 analysis. *Journal of Computational Chemistry*, 25(13), 1605-1612.

612 Phillips, C., Roberts, L., Schade, M., Bazin, R., Bent, A., Davies, N., Moore, R., Pannifer, A.,
613 Pickford, A., Prior, S., Read, C., Scott, A., Brown, D., Xu, B., & Irving, S. (2011).
614 Design and structure of stapled peptides binding to estrogen receptors. *Journal of the*
615 *American Chemical Society*, 133(25).

616 Pike, A. C. W., Brzozowski, A. M., & Hubbard, R. E. (2000). A structural biologist's view of the
617 oestrogen receptor. *Journal of Steroid Biochemistry and Molecular Biology*, 74(5), 261-
618 268.

619 Pitt, J. I. (2013). Mycotoxins. In G. J. Morris & E. M. Potter (Eds.), *Foodborne Infections and*
620 *Intoxications* 4th ed., (pp. 409-418): Academic Press.

621 Rollinger, J. M., Schuster, D., Baier, E., Ellmerer, E. P., Langer, T., & Stuppner, H. (2006).
622 Taspine: bioactivity-guided isolation and molecular ligand-target insight of a potent
623 acetylcholinesterase inhibitor from *Magnolia x soulangiana*. *Journal of Natural Products*,
624 69(9), 1341-1346.

625 Sali, A., & Blundell, T. L. (1993). Comparative protein modelling by satisfaction of spatial
626 restraints. *Journal of Molecular Biology*, 234(3), 779-815.

627 Sonneveld, E., Riteco, J. A., Jansen, H. J., Pieterse, B., Brouwer, A., Schoonen, W. G., & van der
628 Burg, B. (2006). Comparison of in vitro and in vivo screening models for androgenic and
629 estrogenic activities. *Toxicological Sciences*, 89(1), 173-187.

630 Sonoda, M. T., Martinez, L., Webb, P., Skaf, M. S., & Polikarpov, I. (2008). Ligand dissociation
631 from estrogen receptor is mediated by receptor dimerization: Evidence from molecular
632 dynamics simulations. *Molecular Endocrinology*, 22(7), 1565-1578.

633 Spyraakis, F., & Cozzini, P. (2009). How computational methods try to disclose the estrogen

634 receptor secrecy--modeling the flexibility. *Current Medicinal Chemistry*, 16(23), 2987-
635 3027.

636 Tolosa, J., Font, G., Manes, J., & Ferrer, E. (2014). Natural Occurrence of Emerging Fusarium
637 Mycotoxins in Feed and Fish from Aquaculture. *Journal of Agricultural and Food*
638 *Chemistry*, 62(51), 12462-12470.

639 Zinedine, A., Soriano, J. M., Moltó, J. C., & Mañes, J. (2007). Review on the toxicity,
640 occurrence, metabolism, detoxification, regulations and intake of zearalenone: an
641 oestrogenic mycotoxin. *Food and Chemical Toxicology*, 45(1), 1-18.

642

Table 1

Table 1. Docking results on human and rainbow trout ER

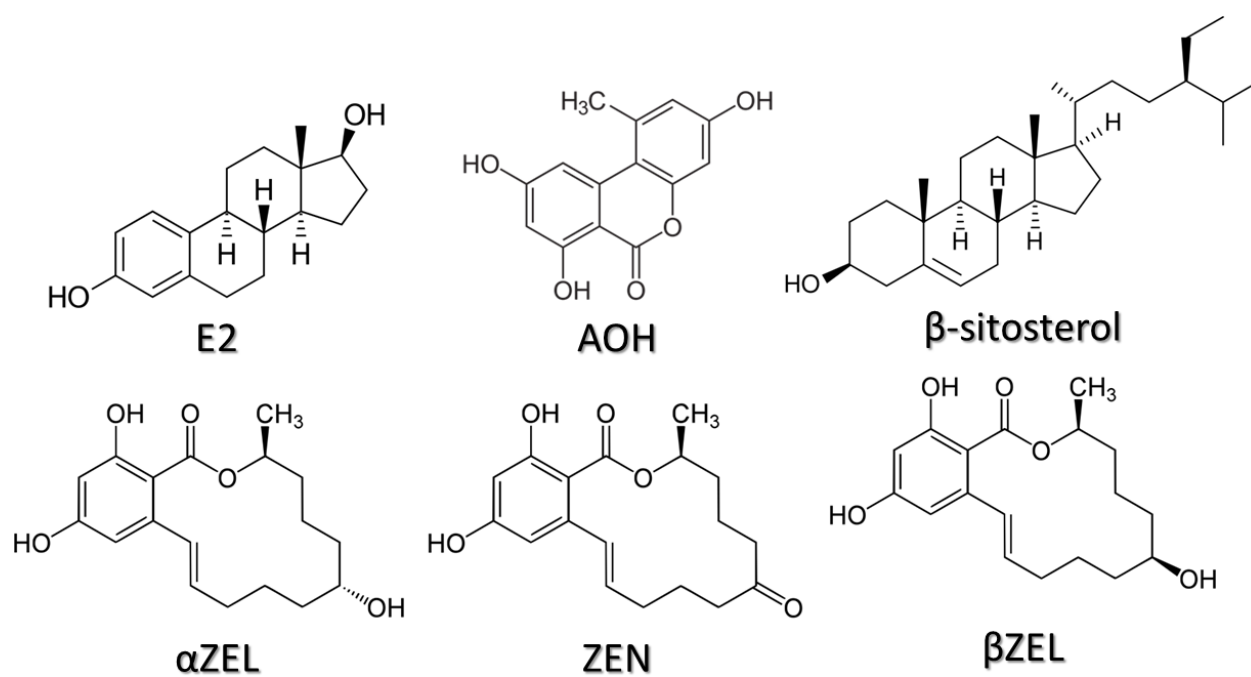
Compound	<i>H. sapiens</i>		<i>O. mykiss</i>	
	Relative estrogenic activity (%)	Relative computed score	Relative estrogenic activity (%)	Relative computed score
E2	100 ^a	1.000	100 ^a	1.000
α ZEL	2.47 ^a	0.945 \pm 0.001	43.33 ^a	0.851 \pm 0.001
ZEN	0.57 ^a	0.912 \pm 0.010	8.39 ^a	0.828 \pm 0.001
β ZEL	0.26 ^a	0.711 \pm 0.008	< 0.01 ^a	0.451 \pm 0.004
β -sitosterol	Inactive ^b	-2.028 \pm 0.303	Inactive ^b	-1.696 \pm 0.312
AOH	0.01 ^c	0.814 \pm 0.002	Not tested yet	0.709 \pm 0.005

^a (Le Guevel and Pakdel 2001)

^b (Matthews et al. 2000)

^c (Lehmann et al. 2006)

Figure 1

**Figure 1.** Chemical structures of molecules accounted in the study.

human and trout ER. Dots indicate conserved amino acids. The residues forming the binding site are highlighted in yellow, while L349/362M and M528/541I are indicated with red boxes. **B.** Superimposition of the 3D structures of human (white) (PDB ID 2YJA) (Phillips et al. 2011) and trout (yellow) ER represented in cartoon. The binding site is represented in mesh. **C.** Superimposition of binding sites of human (white) (PDB ID 2YJA) (Phillips et al. 2011) and trout (yellow) ER. **D.** Comparison between the shape of human (white) (PDB ID 2YJA) (Phillips et al. 2011) and trout (yellow) ER. The shape of the pockets is retraced in cut surface. The reshaping due to the M528/541I mutation is highlighted by the red arrow. **E.** Pharmacophoric differences between human and trout ER. The human pocket is reported and grey mesh indicates the differences of hydrophobic regions found in the two orthologous (i.e. the hydrophobic region found in the human pocket and not in the trout one)

Figure 3

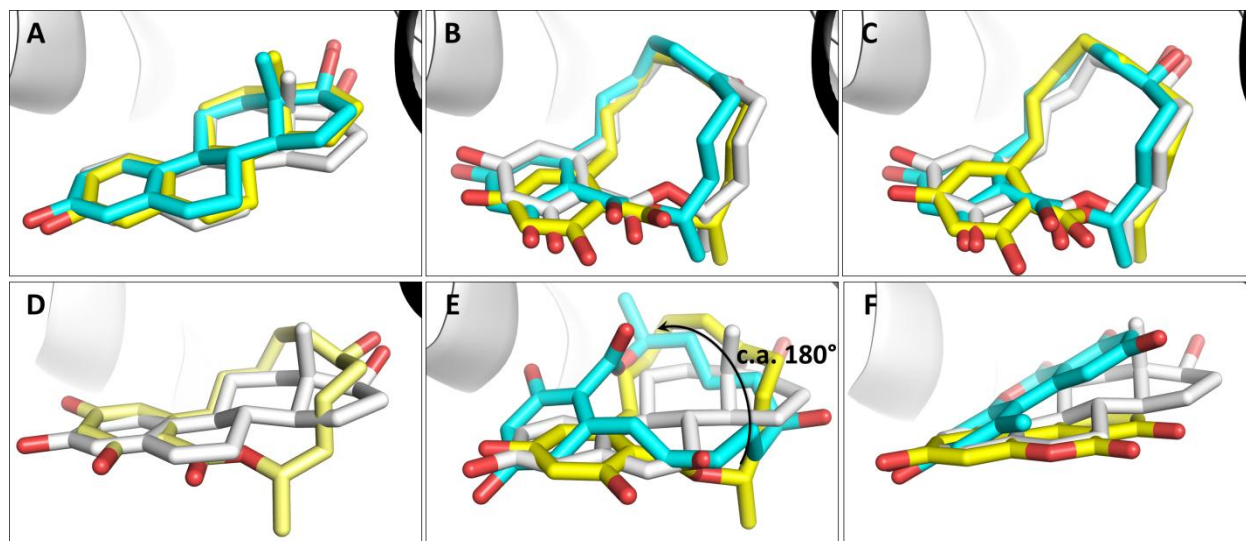


Figure 3. Binding architectures of ligands. Ligands are represented in sticks while ER is represented in cartoon. Unless otherwise specified, the crystallographic poses are reported in white, while in yellow and cyan are reported the computed poses within the human and trout ER, respectively. **A.** Computed pose of E2 in comparison with the binding architecture reported by crystallographic studies (PDB ID 2YJA) (Phillips et al. 2011). **B.** Computed pose of ZEN in comparison with the binding architecture reported by crystallographic studies (PDB ID 5KRC) (Nwachukwu et al. 2017). **C.** Computed pose of α ZEL in comparison with the binding architecture reported by crystallographic studies (PDB ID 4TUZ) (Delfosse et al. 2014). **D.** Superimposition of crystallographic poses of α ZEL (pale yellow) and E2 (white). **E.** Comparison between the crystallographic pose of E2 (PDB ID 2YJA) (Phillips et al. 2011), with the computed poses of β ZEL within the human and trout ER. The black arrow indicates the different orientation the ligand calculated within the trout ER in comparison to the one showed into the human pocket. **F.** Comparison between the crystallographic pose of E2, with the computed poses of AOH within the human and trout ER.

Figure 4

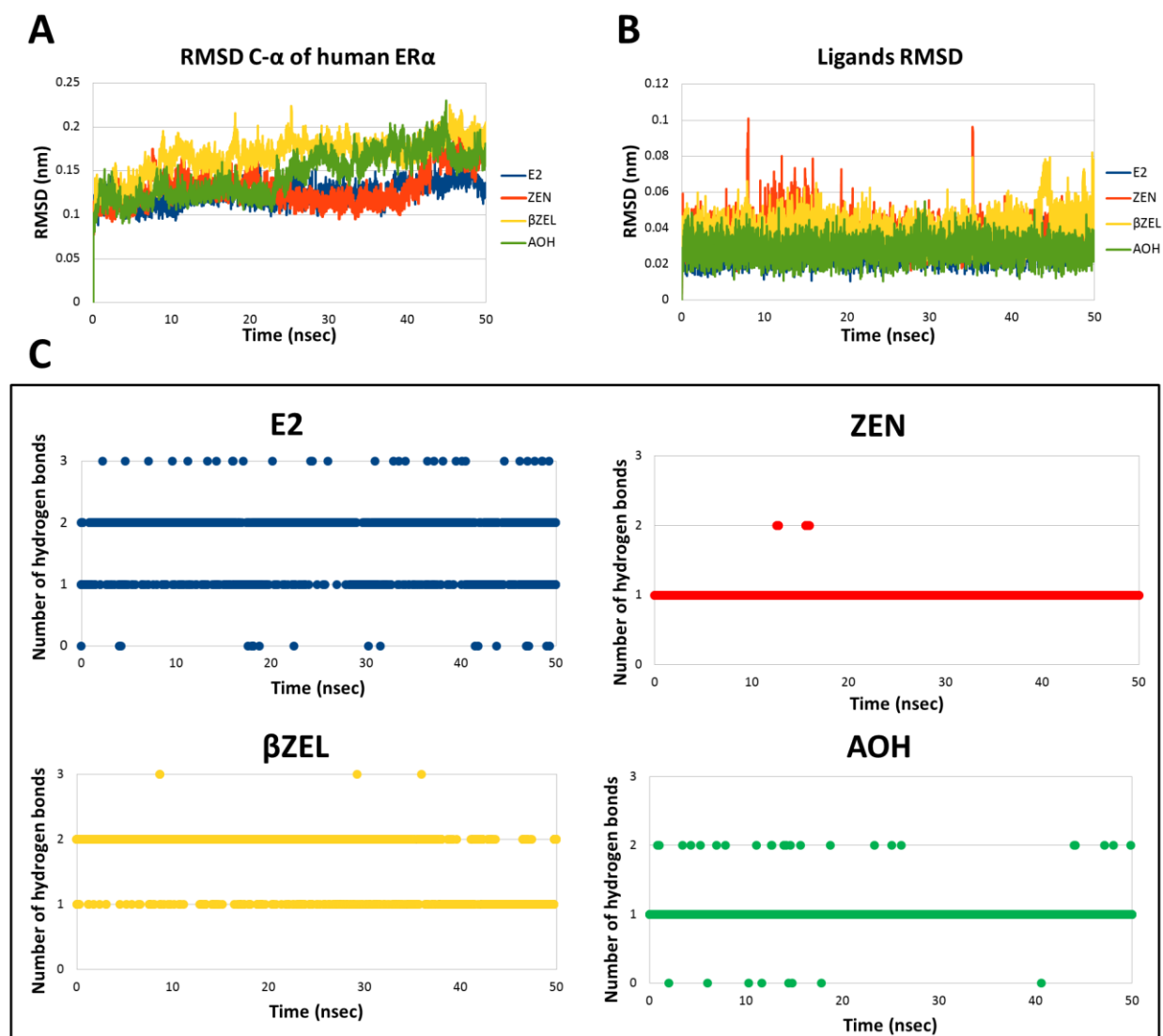


Figure 4. Conformational changes of human ER complexes. **A.** RMSD plot of human ER C- α in complex with E2, ZEN, β ZEL or AOH. **B.** RMSD plot of E2, ZEN, β ZEL or AOH. **C.** Hydrogen bonds blot of human ER in complex with E2, ZEN, β ZEL or AOH.

Figure 5

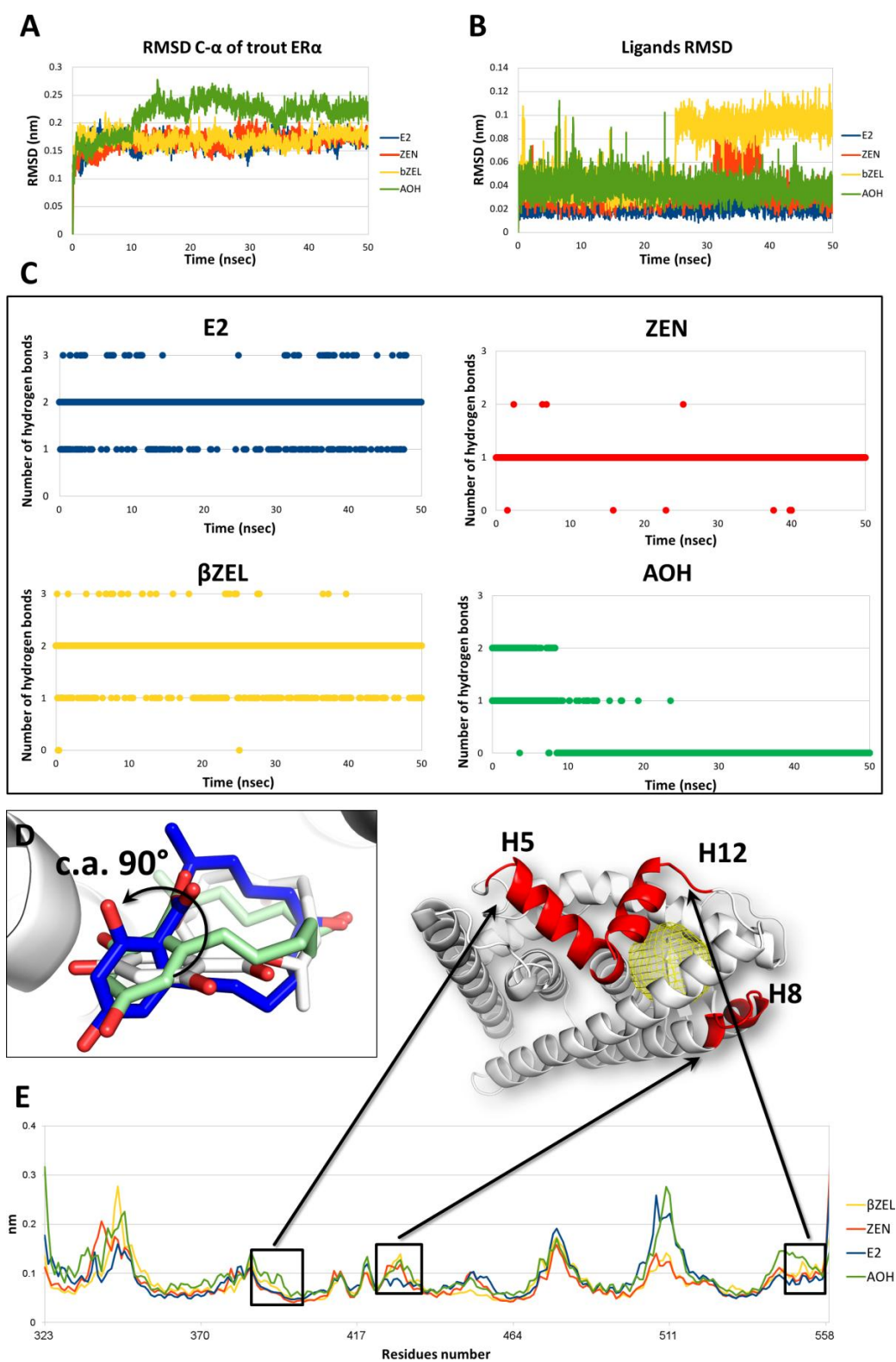


Figure 5. Conformational changes of trout ER complexes. **A.** RMSD plot of trout ER C- α in

complex with E2, ZEN, β ZEL or AOH. **B.** RMSD plot of E2, ZEN, β ZEL or AOH. **C.** Hydrogen bonds blot of trout ER in complex with E2, ZEN, β ZEL or AOH. **D.** Crystallographic pose of ZEN (white) (PDB ID 5KRC) (Nwachukwu et al. 2017) in comparison to the two discrete different poses of β ZEL calculated along the simulation (in green is shown the starting pose, while in blue is shown the pose adopted during the simulation). The black arrow indicates the re-orienting of the molecule during the simulation in respect to the optimal orientation of ZEN. **E.** RMSF plot of residues C- α of trout ER in complex with E2, ZEN, β ZEL or AOH. Black boxes indicate the region found differentially flexible and related to protein activity. The localization of such regions on the ER structure is highlighted in red in the protein representation reported above the plot.

Highlights

- Accounting toxicodynamic aspects may complement mycotoxins risk assessment
- Inter-species differences need to be understood to ameliorate toxicity assessment
- Estrogenicity of zearalenone, its metabolites and alternariol was studied *in silico*
- The diverse toxicodynamic of mycotoxins in human and trout was investigated
- A reliable workflow to characterize dynamic differences among species was shown